Influence of HPGe Detector Energy Resolution on the Results of Isotopic Analysis of Pu with FRAM and MGA Software Codes

A. Rozite

European Commission Joint Research Centre, Ispra, Italy
E-mail: arturs.rozite@ec.europa.eu

Abstract

For plutonium isotopic composition verification, portable HPGe spectrometers accomplished with the isotopic analysis software codes, FRAM and MGA are commonly used by the nuclear safeguards. The codes use absolute branching ratios of radionuclides and intrinsic relative detection efficiency curves for the deconvolution of spectral lines and calculation of isotopic composition [1, 2].
The most important characteristic of HPGe spectrometers in the context of U/Pu composition verification by NDA is the energy resolution of the detector, which basically defines the operability of the isotopic codes. Possible deterioration of the energy resolution caused for example by the degradation of vacuum in the cryostat, or because of the vibrations produced by the cryocooler, may significantly influence the quality of spectrometric results.
The purpose of this work was to establish practical limits on the energy resolution of HPGe detectors suitable for plutonium isotopic composition verification by NDA. To achieve this a Monte Carlo simulation was used. As the result, a set of identical spectra of plutonium but with different energy resolution were created. The spectra of plutonium were simulated using the MCNP6 radiation transport code. The simulation results were validated by the comparison with the real spectrum and analysis on the isotopic composition was performed in two energy windows: from 60 to 230-keV using FRAM and MGA and from 120 to 420-keV using FRAM.
As the result, fitting errors and measurement uncertainties have been described. The conclusion about the possibility to use a simulation approach to describe the operability of software codes depending on the energy resolution of an HPGe detector was made and practical results showing the effects of energy resolution deterioration on the results of the analysis in different energy windows were obtained.

Keywords: Monte Carlo simulation, plutonium, FRAM, MGA

1. Introduction

FRAM and MGA software codes are routinely used for the plutonium isotopic analysis by nuclear safeguards inspectors. The verification activities heavily depend on the availability of HPGe detectors with a good energy resolution. The best results can be achieved using a planar HPGe detector having optimal energy resolution. The importance to have narrow peaks in the spectrum is dictated by the necessity to deconvolute overlapping spectral lines in the X-ray energy region with the highest possible precision. Both codes use nuclear data for the absolute branching ratios and the accuracy of these data is of paramount importance. Although commonly used data are published in JEFF, ENDF and other databases [3], equivalent data were created and refined by the developers of the codes [4].
In the present paper, the Monte Carlo modelling and simulation approach was used to answer the question about the importance of having excellent energy resolution in the spectrum of plutonium measured with an HPGe detector. In this work, a set of spectra of Pu a well-known reference material was simulated using MCNP6 radiation transport code and the energy resolution in the simulated spectra was adjusted in a straight way, by varying of a Gaussian Energy Broadening (GEB) Function of F8 Tally in MCNP.
Alternatively, deliberate deterioration of the energy resolution may be done using physical methods.
JEFF 3.1.1. data were used as a basis to specify energies and branching ratios for the gamma and X-ray peaks in the MCNP input file. Some adjustments were made to get a more realistic spectrum.

In particular, to evaluate the ability of FRAM and MGA software codes to operate outside the normal window of the energy resolution the following was done:

a) Spectrum of a plutonium reference material was measured using a planar HPGe detector having rather optimal energy resolution of 640-eV at 122-keV (740 eV at 208-keV):
b) Equivalent spectrum was simulated using Monte Carlo radiation transport code MCNP6 and validated by the comparison with the real one;
c) Adjusting the energy resolution parameter in MCNP (GEB function of F8 tally) with an increment of 100-eV a set of spectra of CBNM Pu70 standard have been simulated covering the energy resolution range from 545-eV to 1545-eV at 122 keV;
d) Simulated spectra have been processed using isotopic analysis codes FRAM 5.2 and MGA 9.65.
e) The analysis was made in two energy regions: a low-energy region (from 60 to 230-keV) which includes X-ray peaks and which is common for FRAM and MGA codes and in a higher purely gamma-ray energy region (from 120 to 420-keV) which is available in FRAM.

As the result, fitting errors and measurement uncertainties have been described. The conclusion about the possibility to use a simulation approach to describe the operability of software codes depending on the energy resolution of an HPGe detector was made and practical results showing the effects of energy resolution deterioration on the results of the analysis in different energy windows were obtained.

2. Modelling of detector and source

For the measurements, a low-energy germanium detector (LEGe), model GL-1020R [5] with a nominal crystal diameter of 35 mm and height of 20 mm was used. The detector has an aluminium endcap with a beryllium input window. The detector energy resolution is 640-eV at 122-keV (Co-57).
For the given application the detector has slightly worse energy resolution compared to the smaller LEGe or traditional planar HPGe detectors, but also it has a relatively large volume which provides the possibility to get results of the analysis with a better precision also in a high-energy region (from 120 to 420-keV) which can be used in FRAM for the analysis.
The source used for the measurement and in the simulations is the CBNM Pu70 reference material. The source is volumetric and contains 5.8 g of Pu in the form of sintered PuO_2 [6].

The MCNP model of the HPGe detector and the source is shown in Figure 1. The model is a reasonable approximation of the reality and contains all essential parts.
The detector (in pink) is enclosed in a 2 mm thick Cu detector holder. The source (in green) is volumetric and has dimensions of Ø14.7 x 3.7 mm and represents a PuO_2 powder with a density of 10.5 g/cm^3.
Between the source and the detector, there are 2 absorbers: 0.78 mm thick iron absorber (in light blue) which belongs to the CBNM source capsule, and 1.4 mm thick cadmium absorber (in yellow) which was used for the measurements to suppress 59.5-keV line of Am-241.

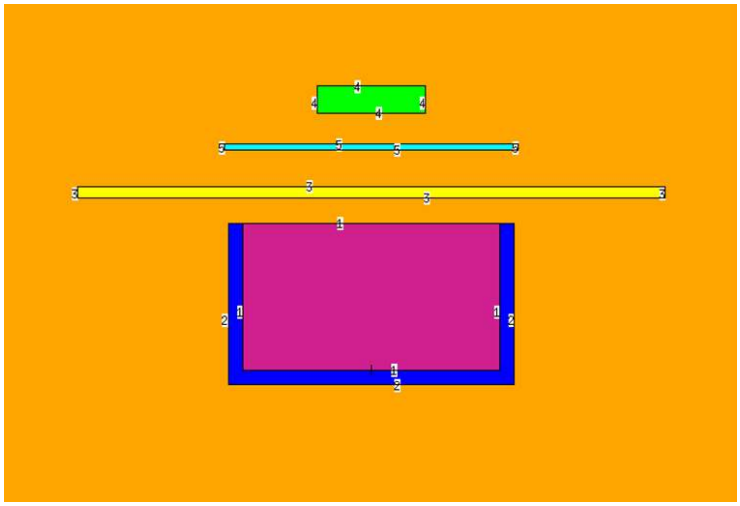

Figure 1 – The geometry of the MCNP simulation.

3. Simulation of plutonium spectrum

CBNM Pu70 reference material source was modelled using nuclear data for the corresponding gamma and X-ray energies and branching ratios of Pu-238, Pu-239, Pu-240, Pu-241 along with short-living daughter isotopes U-237 and Am-241.
For the correct simulation of CBNM Pu70 reference material and to achieve the same spectrum as the measured one used for the comparison, a number of steps described below were performed.

1. From the certified isotopic composition of the CBNM Pu70 reference material, the current isotopic composition was estimated. It was done using the FRAM tool which allows recalculating isotopics accounting to the decay data from the date of certification to the actual date. In FRAM the composition is recalculated by weight.

2. Then accounting for the mass numbers of the isotopes of Pu and Am-241, weight composition was manually recalculated to the atomic composition (Table 1).

3. Then accounting for the half-lives of the isotopes and the atomic composition of the CBNM Pu70 reference material, the multiplication coefficients for given isotopes and their daughters were defined. By these coefficients, the corresponding absolute branching ratios were multiplied.

Table 1. CBNM Pu70 source composition at the certification and measurement dates.

Date	Isotope	Pu-238	Pu-239	Pu-240	Pu-241	Pu-242	Am-241*
20 June 1986	Mass %	0.8458	73.3191	18.2945	5.4634	2.0772	1.1705
	Atom %	0.8506	73.4248	18.2445	5.4257	2.0544	1.1624
9 September 2020	Mass %	0.6776	76.9049	19.1388	1.0978	2.1808	5.6447
	Atom %	0.6812	76.9920	19.0806	1.0899	2.1562	5.6042

** Am-241 concentration is given from the total Pu concentration.*

Multiplication coefficients M_{coef} for the sets of branching intensities for different isotopes were defined according to the equation below

$$M_{coef} = \frac{HL_{Pu-239}}{HL_{Isotope\ X}} \div \frac{CN_{Pu-239}}{CN_{Isotope\ X}}$$

where
HL_{Pu-239} is a half-life of Pu-239;
$HL_{Isotope\ X}$ is a half-life of the isotope of interest;
CN_{Pu-239} is a concentration of Pu-239 in atom %;
$CN_{Isotope\ X}$ is a concentration of the isotope of interest in atom %.

The corresponding X-ray lines branching ratios for U and Np were multiplied by the same coefficients. Pu and Am X-ray lines intensities were found from the comparison with the real spectrum.
The calculation details are shown in Table 2.

Table 2. Calculation matrix.

Radioisotope	Half-life, years	$\frac{HL_{Pu-239}}{HL_{Isotope\ X}}$	CBNM Pu70, atom %	$\frac{CN_{Pu-239}}{CN_{Isotope\ X}}$	M_{coef}
Pu-238	87.7	274.9601	0.6812	113.0211	**2.4328**
Pu-239	24114	1	76.9920	1	**1.0000**
Pu-240	6563	3.674234	19.0806	4.035085	**0.9106**
Pu-241	14.33	1682.763	1.0899	70.63988	**23.8217**
Pu-242	373500	0.064562	2.1562	35.70719	**0.0018**
Am-241	432.8	55.71627	5.6042	13.73828	**4.0555**
U-237					**0.0045% x 23.8217**

4. As mentioned above, only isotopes with relatively short half-lives were used in the simulation and X-ray lines of U and Np were modeled using nuclear data because they are produced together with the decay of corresponding radionuclides; but the intensities of Pu and Am X-ray lines were obtained from the comparison with the measured spectrum, as these X-rays are caused by the interaction of gamma-rays of all radioisotopes with the source material.

5. In order to reduce simulation time the spectral lines below 60-keV including 59.5-keV line of americium were excluded from the simulation and a simplified physics option was used (phys:p 0.0 1 0 0 0 J 0).

6. To get peak-to-background ratio including intensity of a Compton continuum similar to the real one, spectral interferences caused by beta and bremsstrahlung radiation were added. The following methods were used:

a) addition to the MCNP model of a scattering environment around the detector and the source, representing arbitrary physical medium with helium cross-sections and density 1 g/cm^3;
b) addition to the simulated spectrum of a separately simulated continuum produced by monoenergetic 650-keV electron source bombarding 1.5 mm thick aluminium target placed between the source and the detector.

7. First for the comparison, two equivalent spectra of CBNM Pu70 reference material were simulated using JEFF 3.1.1. and ENDF/b-VIII data without corrections. After the comparison, the spectrum simulated using JEFF data was selected as the basis for further modeling due to a simpler representation of X-ray lines. Then, some corrections were made to bring it to a better agreement with the real one. In particular, Np X-ray lines intensities were multiplied by the factor of 0.8 what actually is in good agreement with ENDF data. Several peaks attributed to Am-241 were eliminated and few peaks were added or their intensities were corrected after comparison with the real spectrum. It was done to get equivalent spectral interferences to the real spectrum, so the effects of deterioration of the energy resolution would be equivalent for the real and simulated spectra.

8. For the same reason the branching intensity of 103-keV of Pu-240 was increased by 20 percent. It was done solely to avoid a discrepancy in the result of the analysis between measured and simulated spectrum. This discrepancy can be at least partly attributed to the Gaussian shape of the simulated X-ray peaks which in reality have Lorentzian shape.

9. The number of particles in the MCNP simulation was assigned to get the same intensity of the 208-keV peak for the simulated spectrum as in the real one without applying any correction coefficients for normalization. The real spectrum was measured for 1800 seconds (live time). The results of the simulation are shown in Figure 2 under comparison with the real spectrum.

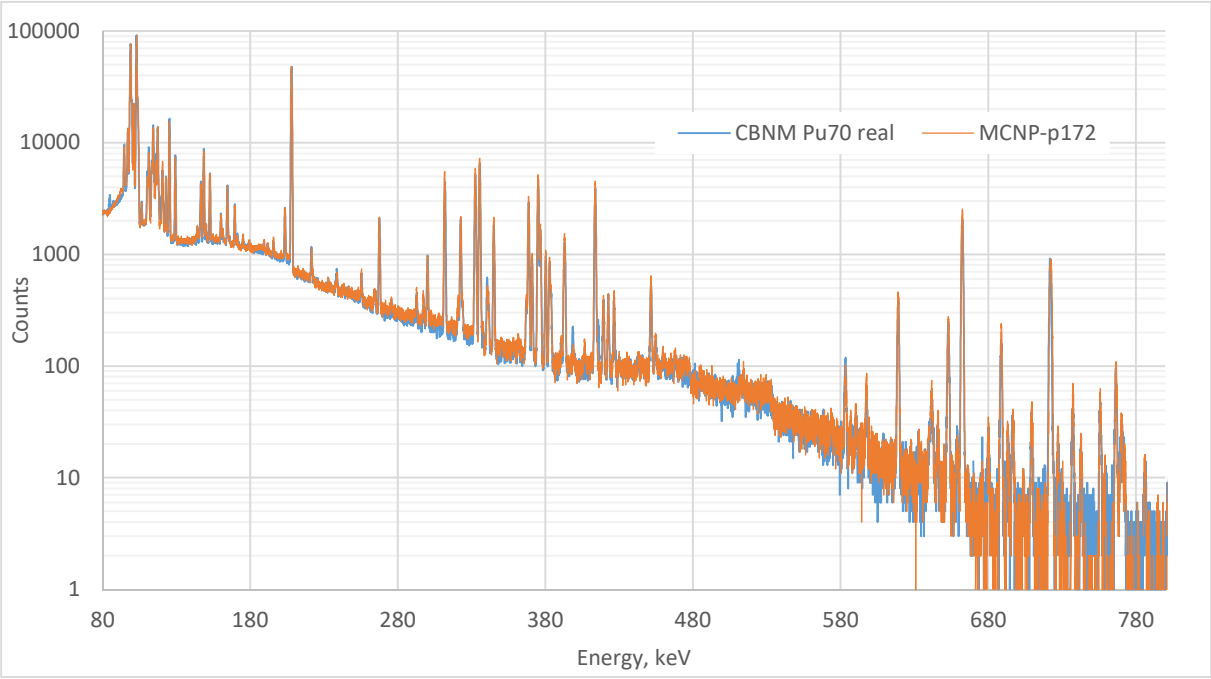

Figure 2 – Comparison of the real (in blue) and simulated (in orange) HPGe detector spectra of CBNM Pu70 standard.

As the most precise results for the plutonium isotopic composition in MGA and FRAM can be obtained using a low-energy region for the analysis, the region which includes many overlapping gamma and X-ray peaks, it was important to achieve the best conformity of the shape of the simulated spectrum shape compared to the measured one. The results of the comparison are shown in Figure 3.

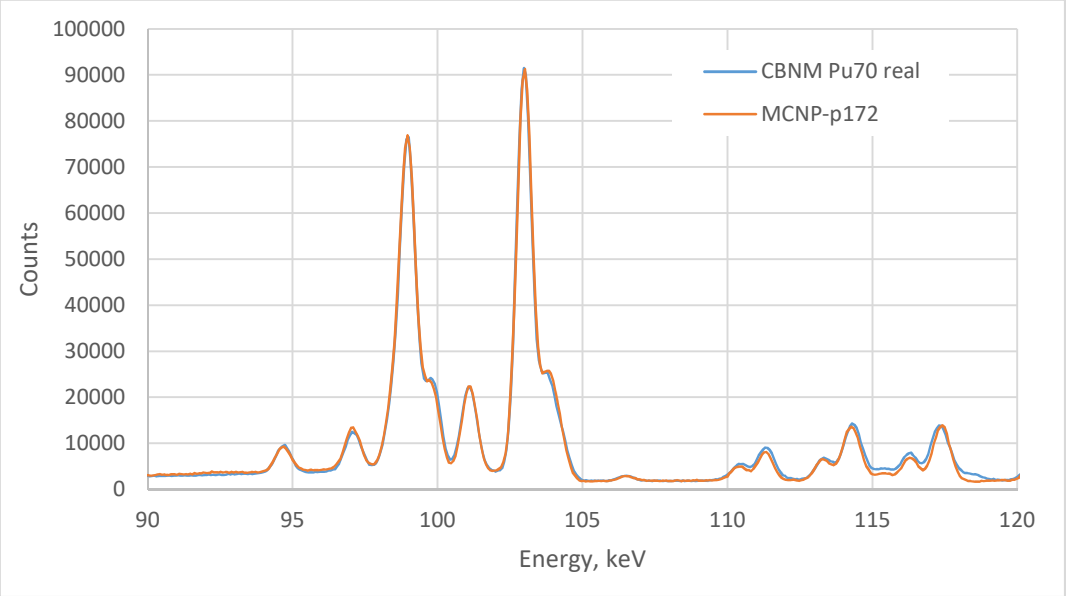

Figure 3 – Comparison of low-energy part of the real (in blue) and simulated (in orange) spectra including 90-110-keV region important for the analysis by the both codes.

The both codes can also use a high-energy region (up to the energy of 1-MeV) for the analysis, but for the best operation in this energy region, a spectrum measured with a coaxial HPGe detector is required. In addition, FRAM offers the possibility to use a medium-energy region (from 120 to 420-keV) for the analysis. In this region, all peaks have a Gaussian shape and good detection efficiency can be achieved with a planar HPGe detector. So operational performance of the FRAM vs, energy resolution was evaluated in this work also for this energy region. In Figure 4 is shown a comparison of the real and simulated spectra for this energy region.

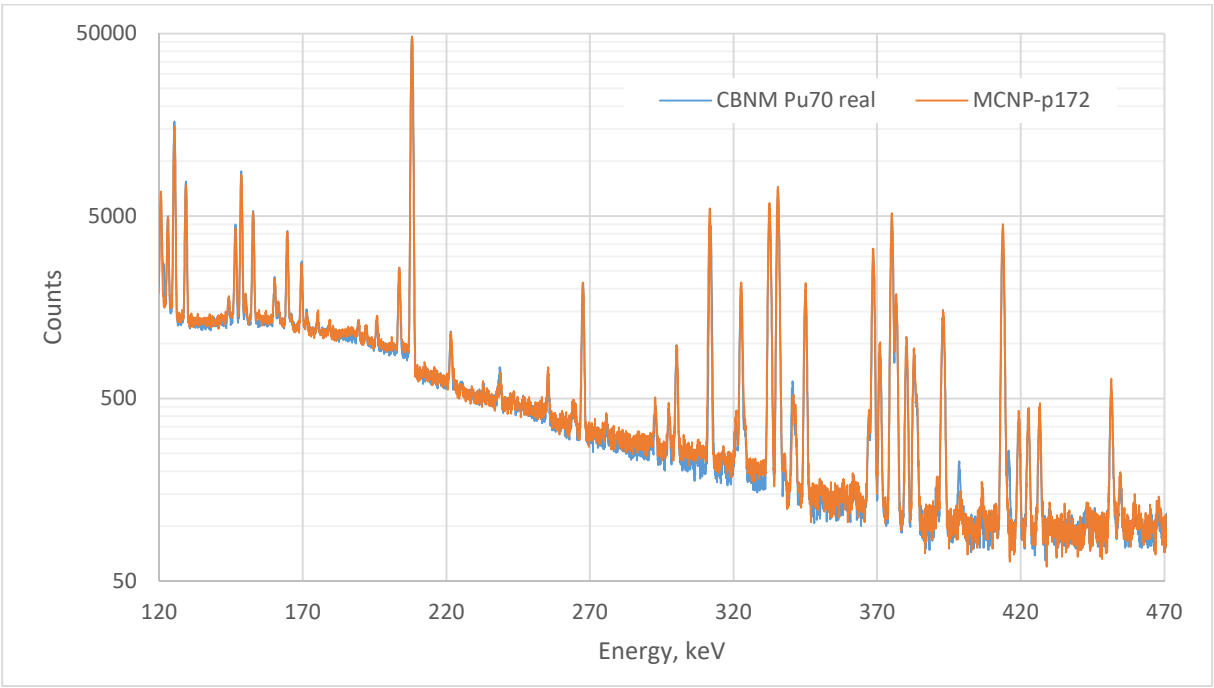

Figure 4 – Comparison of medium-energy part of the real (in blue) and simulated (in orange) spectra including 120-420-keV region used for the analysis by FRAM.

4. Results

4.1. Validation of simulated spectrum using FRAM and MGA

Efficiency curves and quality of fit for the simulated spectrum under comparison with the real one are shown in Figures 5, 6 and 7 below. Both spectra have a similar energy resolution of 640-eV at 122-keV.

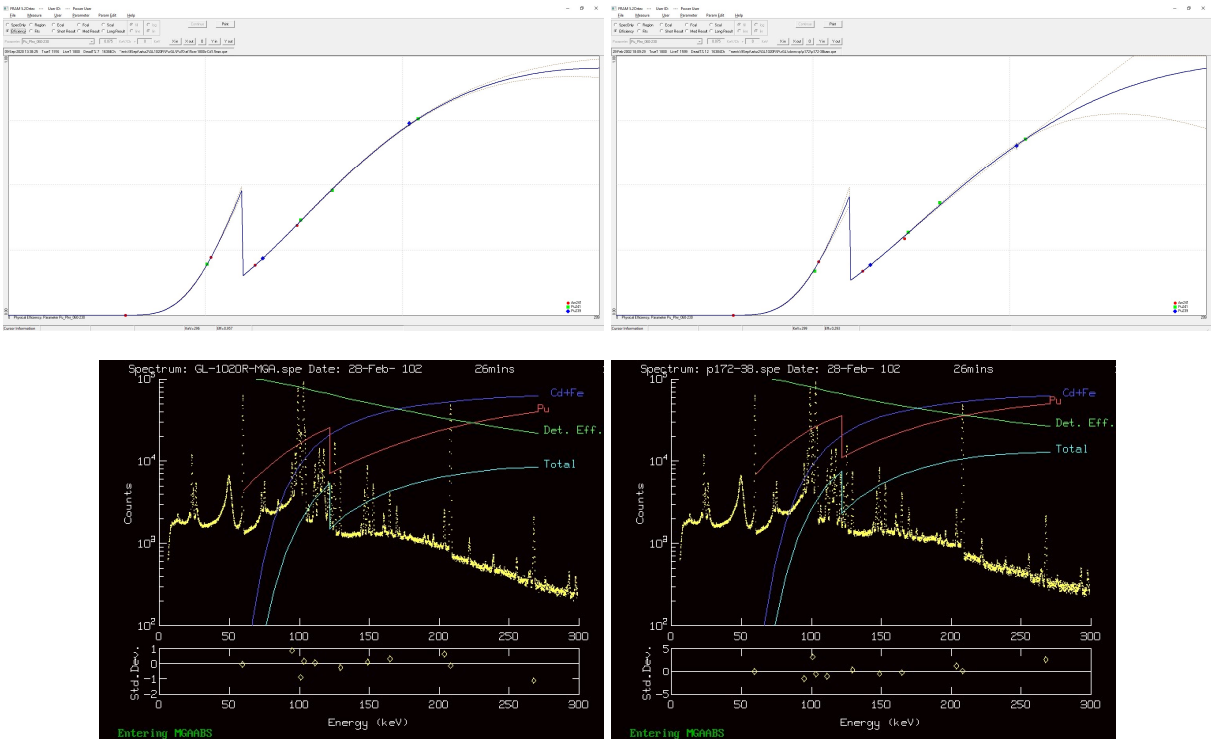

Figure 5 – FRAM and MGA efficiency curves for the real (left) and simulated (right) spectra for low-energy analytical region.

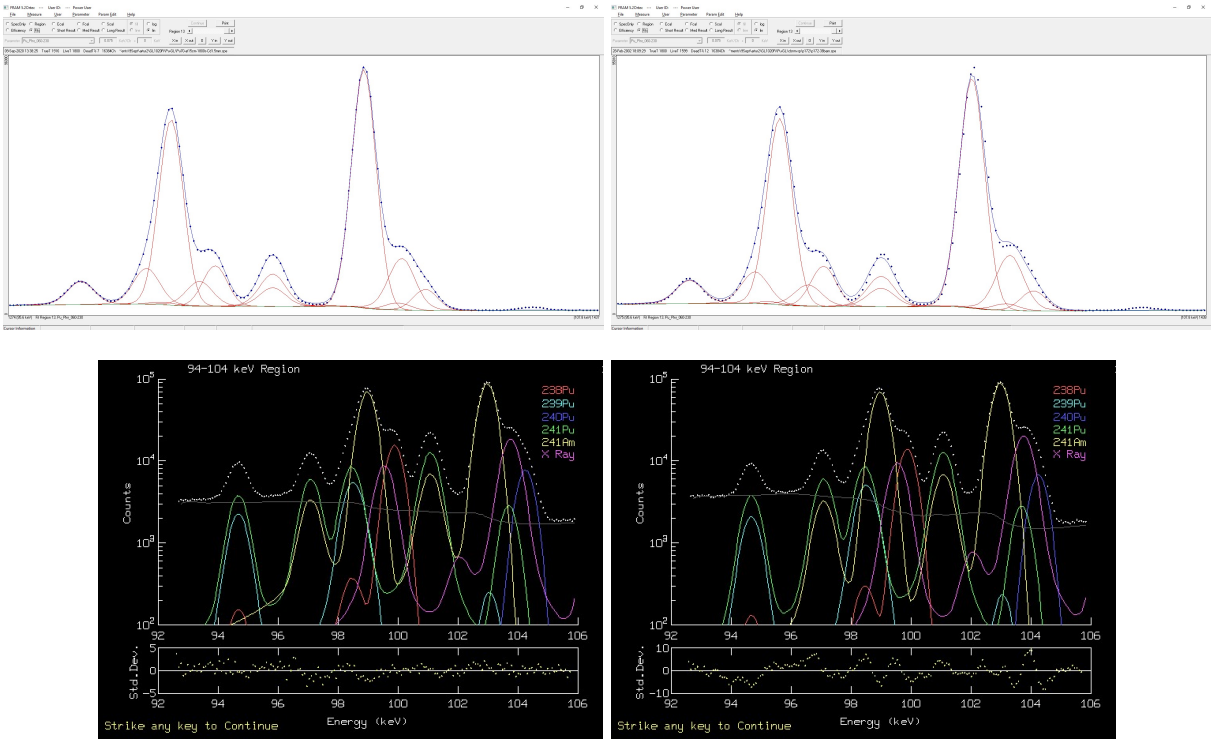

Figure 6 – FRAM and MGA real (left) and simulated (right) spectra fitting (X-ray region).

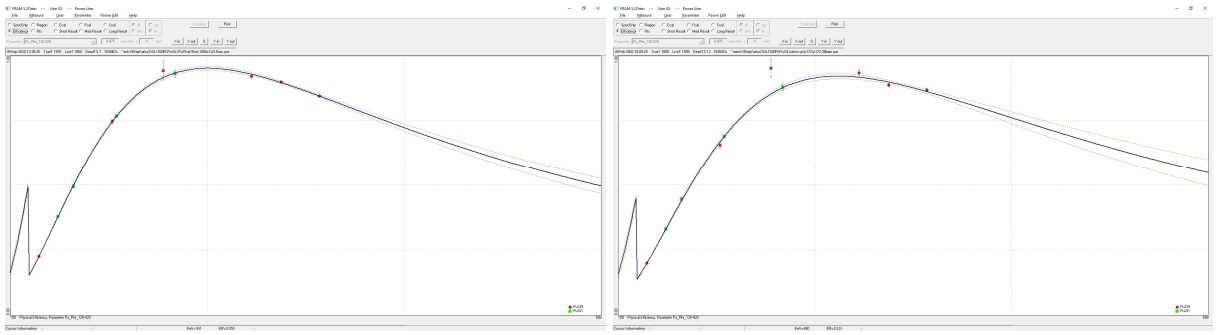

Figure 7 – FRAM efficiency curves for the real (left) and simulated (right) spectra for medium-energy analytical region covering the energy range from 120 to 420-keV.

10. After validation of the simulated spectrum by the comparison with the real one and by the results of the analysis with FRAM and MGA codes, a set of spectra with a different peak's width was simulated. The energy resolution was adjusted using the GEB function of the F8 tally of MCNP covering the range from 545 to 1545-eV at 122-keV with a step of 100-eV. This is illustrated by Figures 8 and 9 below.

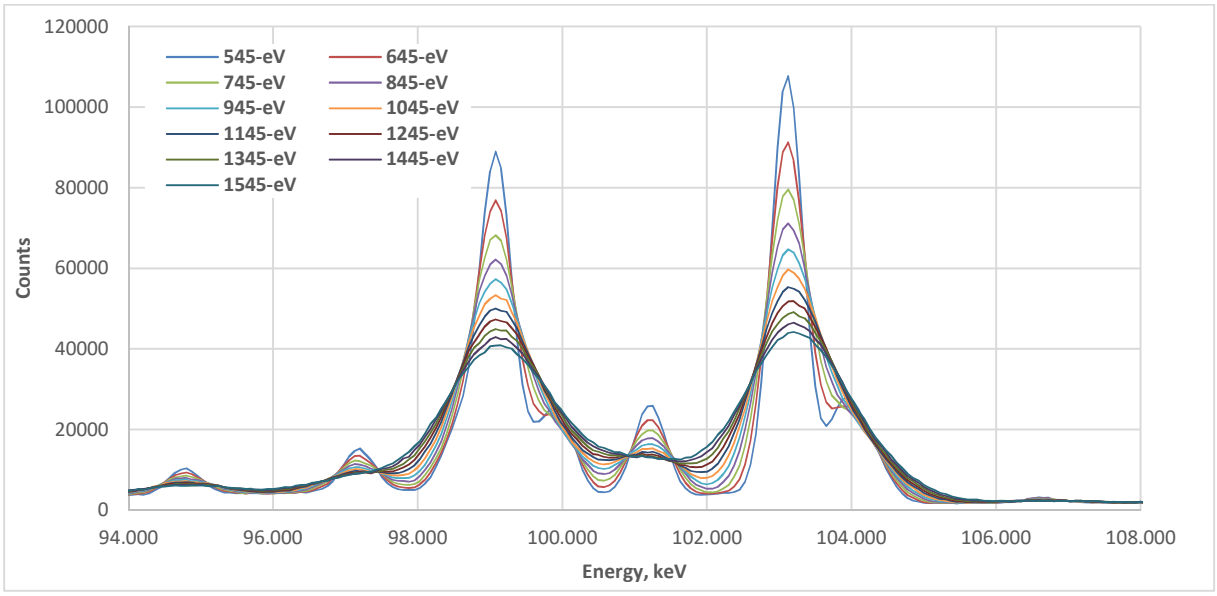

Figure 8 – Simulated spectra of CBNM Pu70 with different energy resolution (X-ray region).

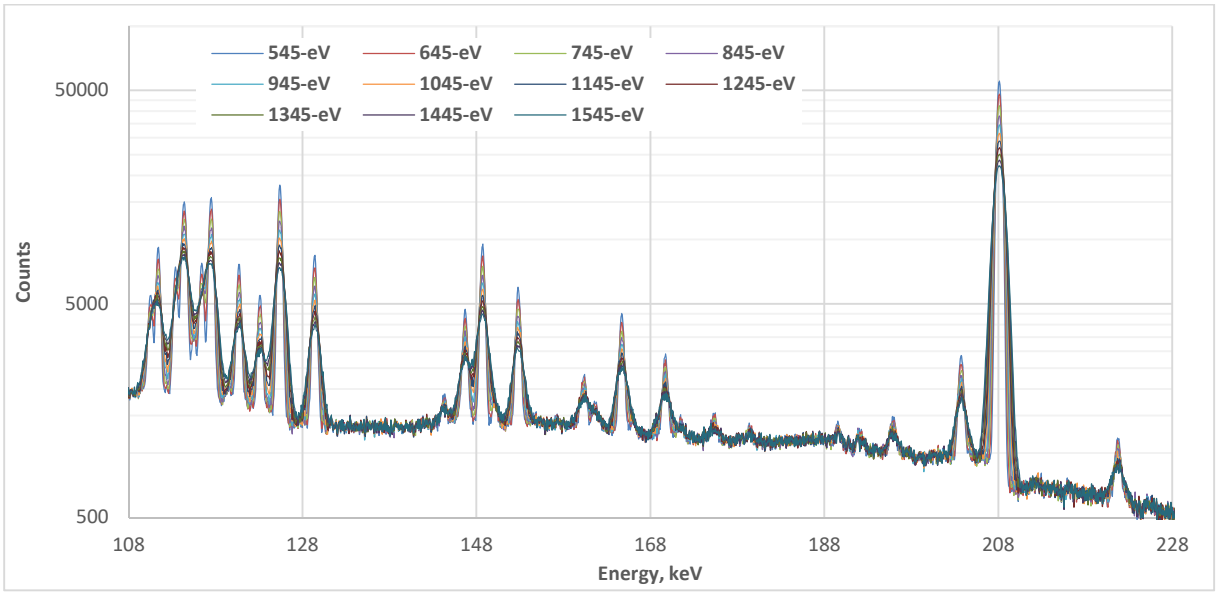

Figure 9 – Simulated spectra of CBNM Pu70 with different energy resolution (108 – 228-keV).

4.2. Results vs. energy resolution

The results of the simulated spectra processing vs. energy resolution are shown in Tables 3–6 below. First, the results obtained for the real spectrum of CBNM Pu70 standard in low- and medium-energy modes by both codes are listed under comparison with the certified value. Then the results are stated for the application of the low-energy method and both codes, and then for the medium-energy method used only in FRAM.

Table 3. Real spectrum with energy resolution of 640-eV at 122-keV.

CBNM Pu70	***Pu-238***	***Pu-239***	***Pu-240***	***Pu-241***	***Pu-242***	***Am-241***
Certified, mass %	0.6776	76.9049	19.1388	1.0978	2.1808	5.6447
Error, 1σ	0.0014	0.0103	0.0091	0.0007	0.0024	0.0564
Measured FRAM	0.6755	77.1937	18.9957	1.0713	2.0638	5.6204
60–230-keV	0.0067	0.2379	0.2397	0.0063	0.0382	0.0330
Measured MGA	0.6584	77.6067	19.0215	1.0888	1.6246	5.5291
60–230-keV	0.0057	0.2483	0.1921	0.00926		0.0415
Measured FRAM	0.6753	77.5902	18.6500	1.0706	2.0139	5.7008
120–420-keV	0.0085	0.4767	0.4943	0.0085	0.0675	0.0521

Table 4. Low-energy mode FRAM.

Results of FRAM version 5.2						
FWHM at 122-keV, eV	***Pu-238***	***Pu-239***	***Pu-240***	***Pu-241***	***Pu-242***	***Am-241***
545	0.6921	77.0002	19.0925	1.1068	2.1084	5.5888
	0.0121	0.519	0.5344	0.0121	0.079	0.0579
645	0.696	77.3162	18.8056	1.1112	2.071	5.6242
	0.0118	0.4844	0.498	0.0109	0.0735	0.0559
745	0.6976	76.2572	19.7173	1.1077	2.2202	5.567
	0.0114	0.5571	0.572	0.0127	0.088	0.0645
845	0.6945	75.2736	20.5718	1.1058	2.3544	5.471
	0.0127	0.6919	0.7128	0.0151	0.1119	0.0757
945	0.6783	74.5072	21.2918	1.0777	2.445	5.4344
	0.0132	0.8002	0.8261	0.017	0.1304	0.0915
1045	0.6688	74.2256	21.5705	1.067	2.4681	5.3568
	0.0138	0.8567	0.8844	0.0191	0.1397	0.1014
1145	0.6504	72.7846	22.8732	1.0345	2.6573	5.2777
	0.0142	0.9095	0.9387	0.0259	0.1544	0.1261
1245	0.6833	73.8581	21.8708	1.0895	2.4982	4.7736
	0.0179	0.7766	0.7893	0.0253	0.1336	0.1306
1345	0.6383	59.5673	33.8143	0.9412	5.0389	3.5978
	0.0427	1.8148	1.88	0.066	0.536	0.1481
1445	0.6053	56.4374	36.3758	0.894	5.6874	3.3539
	0.0428	1.7788	1.8342	0.0677	0.598	0.1451
1545	0.5889	56.2308	36.6606	0.8839	5.6358	3.1779
	0.0451	1.8389	1.8807	0.0733	0.6221	0.1466

Table 5. Low-energy mode MGA.

Results of MGA version 9.65						
FWHM at 122-keV, eV	***Pu-238***	***Pu-239***	***Pu-240***	***Pu-241***	***Pu-242***	***Am241***
545	0.6516	79.5336	17.2213	1.2232	1.3703	6.1700
	0.0226	0.9783	0.7164	0.0402		0.1832
645	0.6369	78.8194	17.9604	1.1913	1.3920	6.0337
	0.0181	0.7882	0.6160	0.0316		0.1460
745	0.6245	78.5761	18.2620	1.1496	1.3879	5.8938
	0.0151	0.6758	0.5497	0.0249		0.1202
845	0.6278	78.8897	17.9441	1.1563	1.3822	6.1076
	0.0136	0.6232	0.5329	0.0219		0.1105
945	0.6934	76.8835	19.2826	1.3452	1.7953	6.9777
	0.0141	0.6381	0.5476	0.0237		0.1165

Table 6. Medium-energy mode FRAM.

Results of FRAM version 5.2						
FWHM at 122-keV, eV	**Pu-238**	**Pu-239**	**Pu-240**	**Pu-241**	**Pu-242**	**Am241**
545	0.6864	77.5586	18.6237	1.0963	2.0351	5.772
	0.0134	0.5074	0.5181	0.011	0.076	0.0929
645	0.6878	77.1902	18.937	1.0967	2.0883	5.7735
	0.0129	0.5345	0.5474	0.011	0.0802	0.0987
745	0.6944	77.3764	18.7608	1.0988	2.0695	5.7616
	0.0126	0.5387	0.5521	0.0115	0.0803	0.0975
845	0.6885	77.055	19.0481	1.1044	2.104	5.7113
	0.0129	0.5924	0.6078	0.0119	0.088	0.1131
945	0.6888	77.0905	19.0114	1.1093	2.1	5.725
	0.013	0.623	0.6394	0.0126	0.0925	0.1156
1045	0.6912	77.2463	18.8591	1.1218	2.0817	5.7417
	0.0129	0.6536	0.6694	0.0132	0.0963	0.133
1145	0.7018	78.0529	18.1135	1.1494	1.9824	5.7565
	0.0131	0.6962	0.7106	0.0139	0.0994	0.1591
1245	0.7076	78.9019	17.3472	1.1696	1.8737	5.7672
	0.0132	0.7467	0.7566	0.0147	0.1027	0.199
1345	0.72	78.8536	17.3489	1.189	1.8885	5.6905
	0.0135	0.7765	0.7863	0.0159	0.1069	0.2174
1445	0.73	79.4497	16.7948	1.2103	1.8152	5.6326
	0.0139	0.8274	0.8379	0.0176	0.1119	0.227
1545	0.7422	80.4581	15.8524	1.2485	1.6988	5.7335
	0.0153	0.9264	0.9297	0.0205	0.1215	0.2849

Summary of the results for Pu-239 concentration is given in Figure 10.

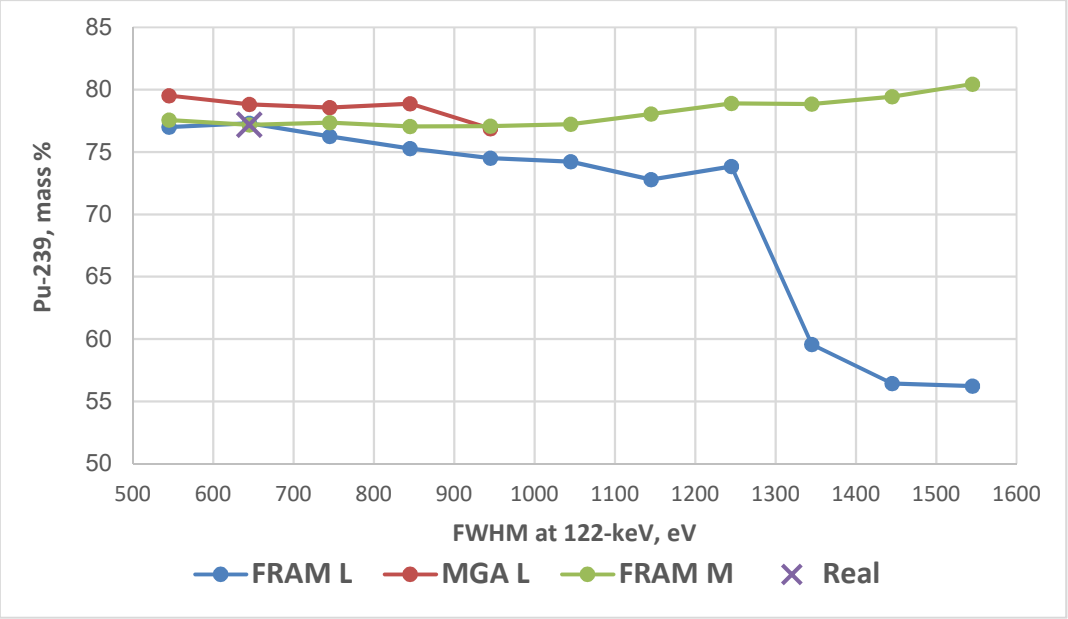

Figure 10 – Pu-239 concentration vs. detector energy resolution, summary of the results.

As it can be seen from Tables 3 – 6, Figures 5 – 7, and Figure 10, the analysis in the low-energy window (FRAM L, MGA L) is in general more sensitive to the energy resolution degradation.
Despite that the intensities of spectral lines are the same for the measured and simulated spectra, the relative errors in the low-energy mode for the simulated spectra are higher by the factor of 2 to 3. The highest discrepancy in the processing of the real and simulated spectra is observed in the fitting of Lorentzian tails of X-ray peaks by the software codes. To achieve the goal of this work in the low-energy region, it is necessary to improve simulation results by simulation of X-ray peaks with Lorentzian shape. For the analysis in the medium-energy region (120-420-keV, FRAM M) in which only Gaussian peaks are present the fitting errors are similar for the real and simulated spectra what gives reliable results for the isotopic composition of Pu vs. energy resolution in this region.

5. Conclusion

The following conclusions are made:

a) FRAM and MGA codes are very useful for the validation of MCNP simulated spectra of plutonium;
b) CBNM Pu standards can be easily modelled in MCNP, self-attenuation of gamma- and X-rays in plutonium is correctly accounted for;
c) For the correct isotopic composition analysis by the software codes in low-energy mode, the best agreement with the real spectra shall be achieved, and therefore simulated X-ray peaks should have Lorentzian shape;
d) Lorentzian shape of X-ray peaks of U, Np, Pu and Am can be modulated using a set of Gaussian probability density functions to create characteristic Lorentzian tails [7];
e) For the analysis in medium-energy mode (120-420-keV FRAM) valid spectra using MCNP were produced. Nevertheless, the branching ratios will be further refined using information available in the software codes and recent nuclear data obtained with microcalorimetry [8].

6. References

[1] R. Gunnink. *MGA: A Gamma-Ray Spectrum Analysis Code for Determining Plutonium Isotopic Abundances.* Volume 1. Methods and Algorithms. UCRL-LR-103220, April 3,1990. https://www.osti.gov/servlets/purl/6738453

[2] Thomas E. Sampson et al. Application Guide to Gamma-Ray Isotopic Analysis Using the FRAM Software. LA-14018, 2003. https://www.lanl.gov/org/ddste/aldgs/sst-training/_assets/docs/App_to_Isotopic_Analysis_using_FRAM.pdf

[3] Evaluated Nuclear Data File (ENDF) Database. https://www-nds.iaea.org/exfor/endf.htm

[4] R. Gunnink, J. E. Evans, and A. L. Prindla. *A REEVALUATION OF THE GAMMA-RAY EMRGIES AND ABSOLUTE BRANCHING INTENSITIES FOR ^{237}U, $^{238, 239, 240, 241}Pu$ and ^{241}Am.* October 11, 1976. https://www.osti.gov/servlets/purl/7320853-5KpBqf/

[5] Low-energy germanium detectors. Datasheet. Mirion Technologies. https://www.mirion.com/products/lege-low-energy-germanium-detector

[6] Robert L. Friar, Thomas E. Sampson. *Plutonium Isotopic Abundance Measurements on CBNM NRM 271 Analyzed with the FRAM and MGA Codes.* Pages 1-3. LA-12309-MS, 1992. https://www.osti.gov/servlets/purl/10140268

[7] Arturs Rozite. *Influence of HPGe Detector Energy Resolution on the Analysis Capabilities of MGAU and FRAM Software Codes.* Proceedings of the IAEA International Workshop on U and Pu Isotopic Analysis by NDA Techniques for Nuclear Safeguards. February 2021 (preprint).

[8] M. D. Yoho, K. E. Koehler, D. T. Becker, D. A. Bennett, M. H. Carpenter, M. P. Croce, J. D. Gard, J. A. B. Mates, D. J. Mercer, N. J. Ortiz, D. R. Schmidt, C. M. Smith, D. S. Swetz, A. D. Tollefson, J. N. Ullom, L. R. Vale, A. L. Wessels, D. T. Vo. *Improved Plutonium and Americium Photon Branching Ratios from Microcalorimeter Gamma Spectroscopy*. 2020.